

Waterlike thermodynamic anomalies in a repulsive-step potential system

N. V. Gribova

*Institute for High Pressure Physics, Russian Academy of Sciences, Troitsk 142190,
Moscow Region, Russia, and Frankfurt Institute for Advanced Studies,
J.W. Goethe-Universität, Ruth-Moufang-Str. 1, D-60438, Frankfurt am Main, Germany*

Yu. D. Fomin and V. N. Ryzhov

Institute for High Pressure Physics, Russian Academy of Sciences, Troitsk 142190, Moscow Region, Russia

Daan Frenkel

*FOM Institute for Atomic and Molecular Physics, Amsterdam,
The Netherlands and Dept. of Chemistry, Univ. of Cambridge, Cambridge, UK*

(Dated: September 16, 2021)

We report a computer-simulation study of the equilibrium phase diagram of a three-dimensional system of particles with a repulsive step potential. The phase diagram is obtained using free-energy calculations. At low temperatures, we observe a number of distinct crystal phases. We show that at certain values of the potential parameters the system exhibits the water-like thermodynamic anomalies: density anomaly and diffusion anomaly. The anomalies disappear with increasing the repulsive step width: their locations move to the region inside the crystalline phase.

PACS numbers: 61.20.Gy, 61.20.Ne, 64.60.Kw

Some liquids (for example, water, silica, silicon, carbon, and phosphorus) show anomalous behavior in the vicinity of their freezing lines [1, 2, 3, 4, 5, 6, 7]. The water phase diagrams have regions where a thermal expansion coefficient is negative (density anomaly), a self-diffusivity increases upon pressuring (diffusion anomaly), and the structural order of the system decreases upon compression (structural anomaly) [6, 7]. The regions where these anomalies take place form nested domains in the density-temperature [6] (or pressure-temperature [7]) planes: the density anomaly region is inside the diffusion anomaly domain, and both of these anomalous regions are inside the broader structurally anomalous region. In the case of water these anomalies are usually related to the anisotropy of the intermolecular potential. However, isotropic potentials are also able to produce density and diffusion anomalies. It is interesting that such potentials may be purely repulsive and can be considered as the simplest models for the water-type anomalies. It has been shown that water-like structural, thermodynamic, and dynamic anomalies can be generated in systems where particles interact via isotropic potentials with two characteristic length scales, with shorter range corresponding to a hard-corelike steep repulsion and longer range representing softer repulsion - potentials in which two preferable interparticle distances compete depending on the thermodynamic conditions of the system [8, 9, 10, 11, 12, 13, 14, 15, 16, 17, 18, 19, 20, 21, 22, 23, 24, 25, 26]. In these studies was found that there is an exception case – the repulsive-step potential – in which no anomalies were reported yet [27]. In this sense, it is very interesting to mention the recent study [28] of evolution of the behavior of the water-like anomalies in the system with a

tunable potential ranging from a ramp potential, which has all mentioned above anomalies to the repulsive-step potential, where no anomalies were found so far [27]. In [28] it was shown that potentials in which two preferred distances are present always exhibit water-like anomalies, but sometimes they are in an inaccessible region, as inside a crystal phase. This is the case for the repulsive-step potential studied in Ref. [27].

However, recently it was shown that water-like anomalies can exist in the systems of particles interacting through the repulsive step potential [29] for some values of the potential parameters.

This potential was introduced in the early work of Hemmer and Stell [8, 9] in order to describe isostructural phase transitions in materials such as Ce or Cs and is the simplest example of a repulsive intermolecular potential that has a region of negative curvature in the repulsive part, a feature that is known to be present in the interatomic potentials of some pure metallic systems, metallic mixtures, electrolytes and colloidal systems. Systems of particles interacting through such pair potentials can possess a rich variety of phase transitions and thermodynamic anomalies, including liquid-liquid phase transitions [30, 31, 32], and isostructural transitions in the solid region [33, 34, 35].

In this sense, the purpose of this paper is straightforward. We will show that the water-like anomalies do exist for the repulsive step potential, but with increasing the width of the repulsive step they move to the inaccessible region inside the crystal phase. The width of the repulsive step of the potential considered in Refs. [27, 28] corresponds exactly to this limiting case.

The repulsive step potential has the form:

$$\Phi(r) = \begin{cases} \infty, & r \leq d \\ \varepsilon, & d < r \leq \sigma \\ 0, & r > \sigma \end{cases} \quad (1)$$

where d is the diameter of the hard core, σ is the width of the repulsive step, and ε its height. In the low-temperature limit $\tilde{T} \equiv k_B T / \varepsilon \ll 1$ the system reduces to a hard-sphere systems with hard-sphere diameter σ , whilst in the limit $\tilde{T} \gg 1$ the system reduces to a hard-sphere model with a hard-sphere diameter d . For this reason, melting at high and low temperatures follows simply from the hard-sphere melting curve $P = cT/\sigma'^3$, where $c \approx 12$ and σ' is the relevant hard-sphere diameter (σ and d , respectively). A changeover from the low- T to high- T melting behavior should occur for $\tilde{T} = \mathcal{O}(1)$. The precise form of the phase diagram depends on the ratio $s \equiv \sigma/d$. For large enough values of s one should expect to observe in the resulting melting curve a maximum that should disappear as $s \rightarrow 1$ [35]. The phase behavior in the crossover region may be very complex, as shown in [29].

In our simulations we have used a smoothed version of the repulsive step potential (Eq. (1)), which has the form:

$$\Phi(r) = \left(\frac{d}{r}\right)^n + \frac{1}{2}\varepsilon(1 - \tanh(k_0(r - \sigma_s))) \quad (2)$$

where $n = 14$, $k_0 = 10$. We have considered the following values of σ_s : $\sigma_s = 1.15, 1.35, 1.55, 1.8$. In Fig. 1 the repulsive step potential is shown along with its smooth version which was used in our Monte-Carlo (MC) and molecular dynamics (MD) simulations.

In the remainder of this paper we use the dimensionless quantities: $\tilde{\mathbf{r}} \equiv \mathbf{r}/d$, $\tilde{P} \equiv Pd^3/\varepsilon$, $\tilde{V} \equiv V/Nd^3 \equiv 1/\tilde{\rho}$. As we will only use these reduced variables, we omit the tildes.

In [29] the phase diagrams of the repulsive step potential system were reported for $\sigma_s = 1.15, 1.35, 1.55$. In the present article we also calculate the phase diagram of the system for $\sigma_s = 1.8$. To determine the phase diagram at non-zero temperature, we performed constant-NVT MD simulations combined with free-energy calculations. In all cases, periodic boundary conditions were used. The number of particles varied between 250, 500 and 864. No system-size dependence of the results was observed. The system was equilibrated for 5×10^6 MD time steps. Data were subsequently collected during $3 \times 10^6 \delta t$ where the time step $\delta t = 5 \times 10^{-5}$.

In order to map out the phase diagram of the system, we computed its Helmholtz free energy using the thermodynamic integration: the free energy of the liquid phase was computed via thermodynamic integration from the dilute gas limit [36], and the free energy of the solid phase was computed by thermodynamic integration to an Einstein crystal [36, 37]. In the MC simulations of solid

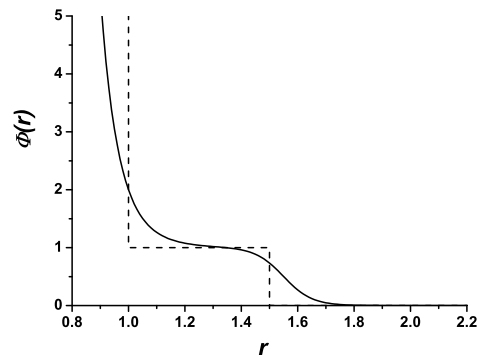


FIG. 1: A repulsive step potential consisting of a hard core plus a finite shoulder (dashed line) ($\varepsilon = 1, \sigma = 1.5$) along with the continuous version of the potential (2) used in the simulations ($\varepsilon = 1, \sigma_s = 1.55$).

phases, data were collected during 5×10^4 cycles after equilibration. To improve the statistics (and to check for internal consistency) the free energy of the solid was computed at many dozens of different state-points and fitted to multinomial function. The fitting function we used is $a_{p,q} T^p V^q$, where T and $V = 1/\rho$ are the temperature and specific volume and powers p and q are connected through $p + q = N$. The value N we used for the most of calculations is 5. For the low-density FCC phase N was taken equal to 4, since we had less data points. The transition points were determined by a double-tangent construction.

The region where we have expected thermodynamic anomalies is situated close to the glassy phase, that means that proper sampling of the phase space can be problematic. To overcome this problem we have used the parallel tempering method [36]. Instead of simulating one system we consider n systems, each running in the NVT ensemble at a different temperature. Systems at high temperatures go easily over potential barriers and systems at low temperatures sample the local free energy minima. The idea of parallel tempering is to put over MD the MC scheme of accepting/rejecting a move, but in our case it would be accepting or rejecting a swap of temperatures between different configurations after each full (equilibration together with sampling) MD run. If the low and high temperatures are far apart, the probability to exchange the configurations is quite low, that is why we use a range of 'intermediate' temperatures between them with a small temperature step. So after running the whole parallel tempering scheme we get a row of systems with subsequent temperatures and each of the systems was sampled several times. For our problem we usually used 8 temperatures and tried to swap them 40 times. This simulation took almost 24 hours running it on 8 processors in parallel at the Joint Supercomputing

Center of Russian Academy of Sciences.

Fig. 2 shows the phase diagrams that we obtain from the free-energy calculations for four different values of σ_s (we included the phase diagrams for $\sigma_s = 1.15, 1.35, 1.55$ for completeness). Fig. 2(a) shows the phase diagram of the system with $\sigma_s = 1.15$. One can see that for the system with $\sigma_s = 1.15$ there are no maxima in the melting curve. In a soft-sphere system described by the potential $1/r^{14}$ a face-centered cubic crystal structure has been reported [38]. However, the addition of a small repulsive step leads to the appearance of the FCC-BCC transition shown in Figs. 2(a).

Fig. 2(b) shows the phase diagram of the system with $\sigma_s = 1.35$ in the $\rho - T$ plane. There is a clear maximum in the melting curve at low densities. The phase diagram consists in two isostructural FCC parts corresponding to close packing of the small and large spheres separated by a sequence of structural phase transitions. This phase diagram was discussed in detail in our previous publication [29]. It is important to mention that there is a region of the phase diagram where we have not found any stable crystal phase. We think that no crystal structure is stable in this density range because of frustration as it was discussed in [29]. In [29] it was shown that the glass transition occurs in this region with $T_g = 0.079$ at $\rho = 0.53$. The apparent glass-transition temperature is above the melting point of the low-density FCC and FCO phases (see Fig. 2(b)). This suggests that the “glassy” phase that we observe is thermodynamically stable. This is rather unusual for one-component liquids. In simulations, glassy behavior is usually observed in metastable mixtures, where crystal nucleation is kinetically suppressed. One could argue that, in the glassy region, the present system behaves like a “quasi-binary” mixture of spheres with diameters d and σ_s and that the freezing-point depression is analogous to that expected in a binary system with a eutectic point: there are some values of the diameter ratio such that crystalline structures are strongly unfavorable and the glassy phase is stable even for very low temperatures. The glassy behavior in the reentrant liquid disappears at higher temperatures.

One can expect the frustration to be even more pronounced if we increase the step size. In Fig. 2(c) we show the phase diagram of the system with the potential (2) for $\sigma_s = 1.55$. One can see that the system also demonstrates low- and high density FCC phases separated by FCC to BCC transitions and the amorphous gap which is much more wider than for $\sigma_s = 1.35$. We did not find any crystal structure between these isostructural phases in our study. The glass transition temperature is $T_g = 0.11091$ at $\rho = 0.5$. One can see that the glassification temperature becomes higher. Given the lack of crystal structure between crystalline phases and the increase of the glass transition temperature one can assume that the frustration effects become higher with the increase of the step width.

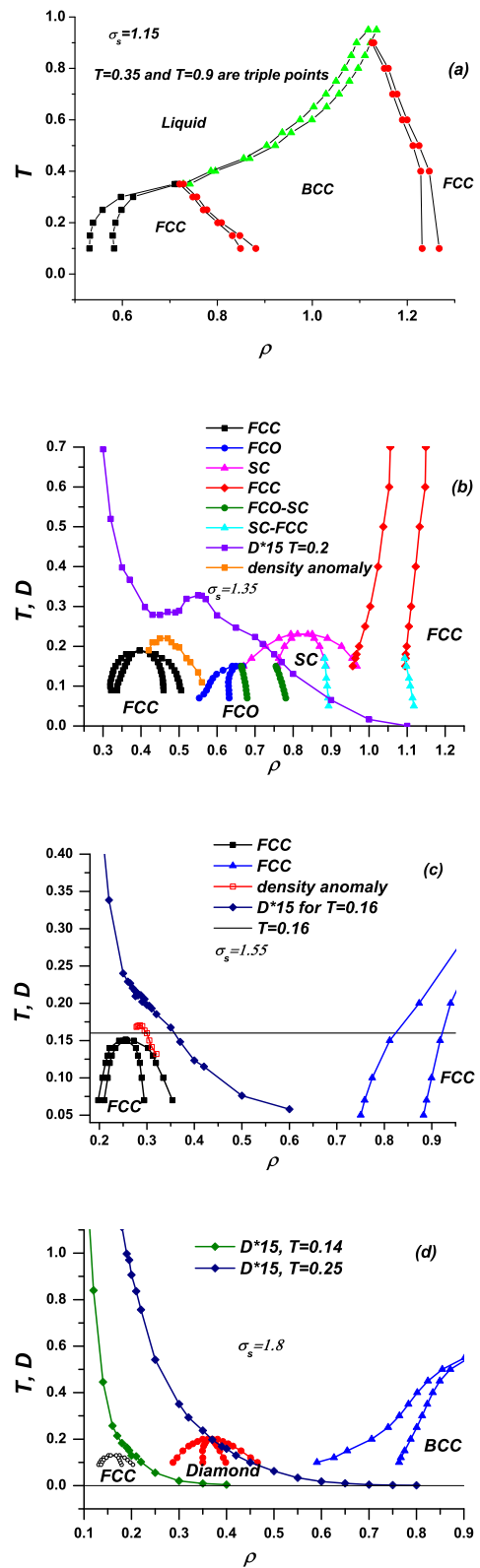


FIG. 2: Phase diagram of the system of particles interacting through the potential (2) with $\sigma_s = 1.15, 1.35, 1.55, 1.8$ in $\rho - T$ plane. In Figs.2 (b-d) it is shown the behavior of the diffusivity as a function of density. In Figs.2 (b-c) we also represent the locations of the minima on the isochores (see Fig. 2.)

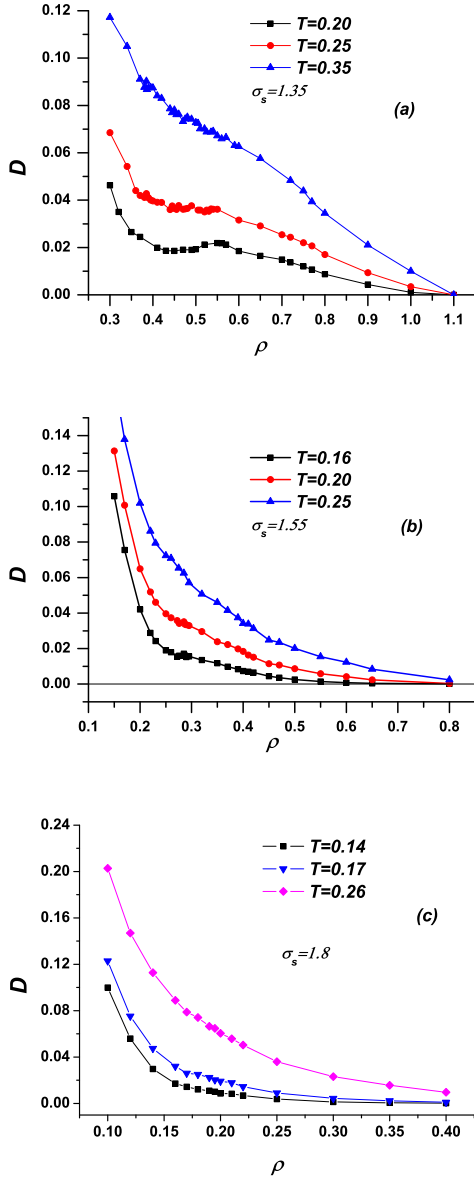


FIG. 3: Diffusion anomaly for $\sigma = 1.35, 1.55, 1.8$.

The phase diagram of the system with $\sigma_s = 1.8$ is shown in Fig. 2(d). One can see that inside the disordered gap in the phase diagram there appears the crystalline phase with diamond structure, however, this phase does not extend over the whole disordered region in the phase diagram.

As it was mentioned above, one can expect the appearance of thermodynamic anomalies in the vicinity of the anomalous points on the phase diagrams of the repulsive-potential system. To check this point, we calculated the isochores and diffusivity for different values of σ_s . In this sense, it is not surprising that there are no thermodynamic anomalies for $\sigma_s = 1.15$. It is known, that

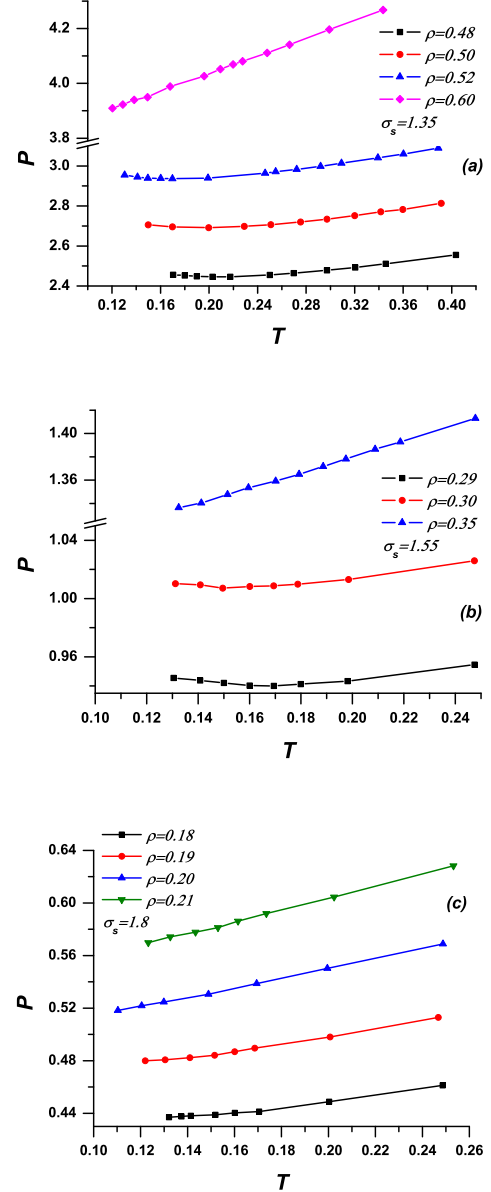


FIG. 4: Density anomaly for $\sigma = 1.35, 1.55, 1.8$.

for normal liquids the diffusivity decreases monotonically with increasing density at constant temperature. In contrast, we have observed in our model, that for a certain values of the potential parameters, for the densities in the vicinity and above the maximum of the melting curve, the diffusivity curve has a bend (see Figs. 3(b-c)). In Figs. 3 the behavior of the diffusivity is shown in more detail for different values of σ_s . One can see that with increasing the width of the repulsive step σ_s the anomaly is becoming less pronounced and disappears for $\sigma_s = 1.8$. It is interesting to note that this value of σ_s corresponds to width of the repulsive step considered in [27, 28] where no anomalies were found for the repulsive step potential.

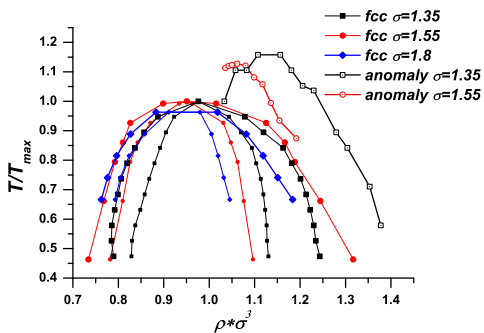


FIG. 5: Re-scaled part of the phase diagram with locations of the minima on the isochores.

The region where the diffusivity anomaly exists almost coincides with a region in which the isochore has a minimum instead of growing monotonically (see Figs. 2(b-c), where the locations of the minima of isochores are shown, and Figs. 4). Using the thermodynamic relation $(\partial P/\partial T)_V = \alpha_P/K_T$, where α_P is a thermal expansion coefficient and K_T is the isothermal compressibility and taking into account that K_T is always positive and finite for systems in equilibrium not at a critical point, one can conclude that there is a range of densities and temperatures where the thermal expansion coefficient α_P is negative.

To elucidate the behavior of the anomalies with increasing the width of the repulsive step of the potential, we re-scaled the parts of the phase diagrams corresponding to the first maximum on the melting curve (see Fig. 2) by multiplying the density by the σ_s^3 and dividing the temperature by T_{max} , where T_{max} is the temperature corresponding to the maximum. In accordance with the qualitative picture depicted above the re-scaled parts of the phase diagrams should coincide. As it is seen in Fig. 5 this is approximately the case for $\sigma_s = 1.35, 1.55, 1.8$. The discrepancies between the curves appear to be because we consider the smoothed version of the repulsive step potential. In Fig. 5 we also show the locations of the minima of the isochores for $\sigma_s = 1.35, 1.55$. One can see that with increasing the width of the repulsive step the line of the minima moves to the melting line and becomes invisible in the metastable region. It should be noticed that this scenario is similar to the one depicted in Ref. 28.

At low densities, we have effectively a liquid consisting of spheres with diameter σ_s , at high densities, the liquid consists of spheres with diameter d . In the “anomalous region” inbetween, our system appears as a mixture of both sorts of particles, and one can expect that in this region structural order should decrease for intermediate values of σ_s . In this case, the entropy of the system should increase with increasing density, and, due to the

thermodynamic relation $(\frac{\partial \rho}{\partial T})_P = \rho^2 (\frac{\partial \rho}{\partial P})_T (\frac{\partial s}{\partial \rho})_T$ [39], one gets the anomalous behavior in this region. This further demonstrates that our model shows a quasi-binary behavior.

In summary, we have performed the extensive computer simulations of the phase behavior of systems described by the soft, purely repulsive step potential (2) in three dimensions. We find a surprisingly complex phase behavior. We argue that the evolution of the phase diagram may be qualitatively understood by considering this one-component system as a quasi-binary mixture of large and small spheres. Interestingly, the phase diagram includes two crystalline FCC domains separated by a sequence of the structural phase transitions and a reentrant liquid that becomes amorphous at low temperatures. The water-like anomalies (density anomaly and diffusion anomaly) were found in the reentrant liquid for $\sigma_s = 1.35, 1.55$. The anomalies disappear with increasing the repulsive step width: their locations move to the region inside the crystalline phase in the vicinity of the maximum on the melting line.

We thank S. M. Stishov and V. V. Brazhkin for stimulating discussions. N.G. thanks A. Arnold for introduction to parallel computing and valuable remarks. N.G. and Y.F. thank the Joint Supercomputing Center of Russian Academy of Sciences for computational power. The work was supported in part by the Russian Foundation for Basic Research (Grant No 08-02-00781) and the Fund of the President of Russian Federation for Support of Young Scientists (MK-2905.2007.2).

-
- [1] P. Debenedetti, J. Phys.: Condens. Matter **15**, R1669 (2003).
 - [2] S. V. Buldyrev, G. Franzese, N. Giovambattista, G. Malescio, M. R. Sadr-Lahijany, A. Scala, A. Skibinsky, and H. E. Stanley, Physica A **304**, 23 (2002).
 - [3] C. A. Angell, Annu. Rev. Phys. Chem. **55**, 559 (2004).
 - [4] P. G. Debenedetti, *Metastable Liquids: Concepts and Principles* (Princeton University Press, Princeton, 1998).
 - [5] V. V. Brazhkin, S. V. Buldyrev, V. N. Ryzhov, and H. E. Stanley [eds], *New Kinds of Phase Transitions: Transformations in Disordered Substances* [Proc. NATO Advanced Research Workshop, Volga River] (Kluwer, Dordrecht, 2002).
 - [6] J. R. Errington and P. G. Debenedetti, Nature (London) **409**, 18 (2001).
 - [7] P.A. Netz, F.V. Starr, H.E. Stanley, and M.C. Barbosa, J. Chem. Phys. **115**, 318 (2001).
 - [8] P. C. Hemmer and G. Stell, Phys. Rev. Lett. **24**, 1284(1970).
 - [9] G. Stell and P. C. Hemmer, J. Chem. Phys. **56**, 4274 (1972).
 - [10] G. Malescio, J. Phys.: Condens. Matter **19**, 07310 (2007).
 - [11] E. Velasco, L. Mederos, G. Navascues, P. C. Hemmer, and G. Stell, Phys. Rev. Lett. **85**, 122 (2000).
 - [12] P. C. Hemmer, E. Velasco, L. Mederos, G. Navascues, and

- G. Stell, *J. Chem. Phys.* **114**, 2268 (2001).
- [13] M. R. Sadr-Lahijany, A. Scala, S. V. Buldyrev and H. E. Stanley, *Phys. Rev. Lett.* **81**, 4895 (1998).
- [14] M. R. Sadr-Lahijany, A. Scala, S. V. Buldyrev and H. E. Stanley, *Phys. Rev. E* **60**, 6714 (1999).
- [15] P. Kumar, S. V. Buldyrev, F. Sciortino, E. Zaccarelli, and H. E. Stanley, *Phys. Rev. E* **72**, 021501 (2005).
- [16] L. Xu, S. V. Buldyrev, C. A. Angell, and H. E. Stanley, *Phys. Rev. E* **74**, 031108 (2006).
- [17] E. A. Jagla, *J. Chem. Phys.* **111**, 8980 (1999); E. A. Jagla, *Phys. Rev. E* **63**, 061501 (2001).
- [18] F. H. Stillinger and D. K. Stillinger, *Physica (Amsterdam)* **244A**, 358 (1997).
- [19] A. B. de Oliveira, P. A. Netz, T. Colla, and M. C. Barbosa, *J. Chem. Phys.* **124**, 084505 (2006).
- [20] A. B. de Oliveira, P. A. Netz, T. Colla, and M. C. Barbosa, *J. Chem. Phys.* **125**, 124503 (2006).
- [21] A. B. de Oliveira, M. C. Barbosa, and P. A. Netz, *Physica A* **386**, 744 (2007).
- [22] J. Mittal, J. R. Errington, and T. M. Truskett, *J. Chem. Phys.* **125**, 076102 (2006).
- [23] H. M. Gibson and N. B. Wilding, *Phys. Rev. E* **73**, 061507 (2006).
- [24] P. Camp, *Phys. Rev. E* **71**, 031507 (2005).
- [25] A. B. de Oliveira, G. Franzese, P. A. Netz, and M. C. Barbosa, *J. Chem. Phys.* **128**, 064901 (2008).
- [26] L. Xu, S. Buldyrev, C. A. Angell, and H. E. Stanley, *Phys. Rev. E* **74**, 031108 (2006).
- [27] A. B. de Oliveira, P. A. Netz, and M. C. Barbosa, *Euro. Phys. J. B* **64**, 481 (2008).
- [28] A. B. de Oliveira, P. A. Netz, and M. C. Barbosa, arXiv:0804.2287v1.
- [29] Yu. D. Fomin, N. V. Gribova, V. N. Ryzhov, S. M. Stishov, and Daan Frenkel, *J. Chem. Phys.* **129**, 064512 (2008).
- [30] V. N. Ryzhov and S. M. Stishov, *Zh. Eksp. Teor. Fiz.* **122**, 820 (2002)[*JETP* **95**, 710 (2002)].
- [31] V. N. Ryzhov and S. M. Stishov, *Phys. Rev. E* **67**, 010201(R) (2003).
- [32] Yu. D. Fomin, V. N. Ryzhov, and E. E. Tareyeva, *Phys. Rev. E* **74**, 041201 (2006).
- [33] D. A. Young and B. J. Alder, *Phys. Rev. Lett.* **38**, 1213 (1977); D. A. Young and B. J. Alder, *J. Chem. Phys.* **70**, 473 (1979).
- [34] P. Bolhuis and D. Frenkel, *J. Phys.: Condens. Matter* **9**, 381 (1997).
- [35] S. M. Stishov, *Phil. Mag. B* **82**, 1287 (2002).
- [36] Daan Frenkel and Berend Smit, *Understanding molecular simulation (From Algorithms to Applications)*, 2nd Edition (Academic Press), 2002.
- [37] D. Frenkel and A. J. Ladd, *J. Chem. Phys.* **81**, 3188 (1984).
- [38] R. Agrawal and D.A. Kofke, *Phys. Rev. Lett.* **74**, 122 (1995).
- [39] R. M. Lynden-Bell and P. G. Debenedetti, *J. Phys. Chem. B* **109**, 6527 (2005).